Science of Sintering, **49** (2017) 235-246

doi: https://doi.org/10.2298/SOS1703235O

UDK 666.3-127, 663.12, 622.785

Formation of Porous Wollastonite-based Ceramics after Sintering With Yeast as the Pore-forming Agent

Nina Obradović[1,*], Suzana Filipović[1], Jelena Rusmirović[2], Georgeta Postole[3], Aleksandar Marinković[4], Danka Radić[5], Vesna Rakić[5], Vladimir Pavlović[1,5], Aline Auroux[3]

[1]Institute of Technical Sciences of SASA, 11000 Belgrade, Serbia
[2]Innovation center, Faculty of Technology and Metallurgy, University of Belgrade, 11120 Belgrade, Serbia
[3]IRCELYON - UMR 5256 CNRS/Université Lyon1, 69626 Villeurbanne Cedex France
[4]Faculty of Technology and Metallurgy, University of Belgrade, 11120 Belgrade, Serbia
[5]Faculty of Agriculture, University of Belgrade, 11000 Belgrade, Serbia

Abstract:

In this paper, synthesis of porous wollastonite-based ceramics was reported. Ceramic precursor, methylhydrocyclosiloxane, together with micro-sized $CaCO_3$, was used as starting material. After 20 min of ultrasound treatment, and calcination at 250 ^oC for 30 min, yeast as a pore-forming agent was added to the as-obtained powders. Sintering regime was set up based on the results obtained by differential thermal analysis. Prepared mixture was pressed into pallets and sintered at 900 ^oC for 1 h. After the sintering regime, porous wollastonite-based ceramics was obtained. The phase composition of the sintered samples as well as microstructures was analyzed by X-ray diffraction method and SEM. In a batch test, the influence of pH, contact time and initial ion concentration on adsorption efficiency of As^{+5}, Cr^{+6}, and phosphate ions on synthesized wollastonite-based ceramics were studied. Time-dependent adsorption was best described by pseudo-second-order kinetic model and Weber-Morris model that predicted intra-particle diffusion as a rate-controlling step of overall process. High adsorption capacities 39.97, 21.87, and 15.29 mgg^{-1} were obtained for As^{+5}, Cr^{+6}, and phosphate ions, respectively.

Keywords: *Yeast, Sintering, Porous wollastonite ceramics.*

1. Introduction

Four types of compounds could be formed in the CaO-SiO_2 system: monocalcium silicate, known as wollastonite ($CaSiO_3$), dicalcium silicate, known as larnite (Ca_2SiO_4), tricalcium silicate (Ca_3SiO_5), and tricalcium disiliconheptaoxide ($Ca_3Si_2O_7$). Different calcium silicate could be synthesized, depending on the molar ratio of starting materials [1].

Wollastonite is widely used in ceramic fabrication, as a high frequency insulator, filler material in resins and plastics, in civil construction, metallurgy, as paint and frictional

*) Corresponding author: nina.obradovic@itn.sanu.ac.rs (Dr. Nina Obradović)

products regarding to its properties, such as low dielectric constant, low dielectric loss, thermal stability, low thermal expansion and low thermal conductivity [2–4]. Furthermore, wollastonite owns possibility of applying as the medical material for artificial bones and dental roots due to biocompatibility, bioactivity and degradability [5, 6].

On the other hand, porous materials find nowadays many applications as final products and in several technological processes regarding their special properties and features that usually cannot be achieved by their conventional dense shape.

Macro-porous materials have a wide application in many human life segments including porous ceramics for water purification. Recently, an increasing need for porous ceramics, especially for environments where high temperatures, extensive wear and corrosive media are involved, have appeared. The many advantages of using porous ceramics are observed such as high melting point, tailored electronic properties, high corrosion, and wear resistance [7]. One of the ways to obtain porous ceramic is addition of either inorganic or organic pore-forming agents. Inorganic pore-forming agents are ammonium carbonate, ammonium bicarbonate and ammonium chloride salts or other high temperature decomposable inorganic carbon such as graphite, coal ash, etc.; organic pore-forming agent include natural fibers, polymers, such as sawdust, shell and corn flour, starch, polystyrene (PS), polymethyl methacrylate (PMMA), and yeast [8–10].

Wollastonite preparation is very important in scientific terms because of all mentioned potential applications. It has been synthesized using a few techniques such as precipitation, sol-gel, solid-state reaction, etc. All of them require high temperatures of sintering 950-1400 ^{o}C [11–14]. Another, very useful method for obtaining wollastonite ceramics is synthesis from preceramic precursors. Siloxanes, as a source of silicon, represent often investigated type of preceramic polymers. Polymers are subjected to transformation into ceramics during heat treatment [15]. This method offers some advantages such as possibility of combining shaping and synthesis of ceramics, in a very easy way and with lower applied temperatures, up to 900 ^{o}C in wollastonite preparation.

In this study, porous wollastonite-based ceramics synthesized by addition of yeast, as an organic pore-forming agent already used for the synthesis of ceramic materials, were investigated [16–18]. The aim of this paper was to demonstrate influence of yeast on phase composition and microstructure. The objective of the present work was to use wollastonite - based ceramics for the removal of As^{+5}, Cr^{+6}, and phosphate ions from aqueous solutions. The studies have been carried out at various concentrations, retention times and pH.

2. Experimental procedure

2.1. Materials

For wollastonite preparation, $CaCO_3$ (Sigma-Aldrich, p.a.), isopropyl alcohol (Sigma-Aldrich, p.a.) and methylhydrocyclosiloxane (ABCR, 100 g) were used. All chemicals used in this study were reagent grade and used as received. Deionized water (DIW), resistivity 18 MΩcm, was used as solvent. The As^{+5}, Cr^{+6}, and phosphate stock solutions were prepared with DIW using $Na_2HAsO_4{\cdot}7H_2O$, $K_2Cr_2O_7$, and K_2HPO_4 (Sigma-Aldrich). Ultra pure HNO_3 acid was supplied from Fluka.

2.2. Adsorbents preparation

2.2.1. Yeast isolation

Yeast was isolated from soil sample (experimental field Radmilovac, Serbia) using serial dilution method. YPD (*yeast extract–peptone-dextrose*) medium which consists of 1 % yeast extract, 2 % peptone, and 2 % dextrose, was used for the isolation at the temperature of

28 ºC/48 h [19]. 100 ml of YPD medium was inoculated by the yeast isolate. Incubation was performed in orbital shaker (Biosan-20KS, Latvia) for two days at the temperature of 28 ºC and at 150 rpm. The final yeast concentration in medium was $1 \cdot 10^8$ CFU ml^{-1}, which corresponds to the absorbance of 0.5 at 780 nm (T70 UV / VIS Spectromer, PG Instruments Ltd., UK).

2.2.2. Synthesis of wollastonite-based adsorbent

Wollastonite-based adsorbents were synthesized in two-step process. In the first step 7.7905 g siloxane (methylhydrocyclosiloxane) was dissolved in 100 ml isopropyl alcohol at magnetic stirrer for 10 min. 12.9220 g of micro-sized $CaCO_3$ was added and mixed for another 10 min, followed by ultrasound treatment for 20 min and drying overnight at 80 ^oC. The obtained paste was calcined in furnace at 250 ^oC during 30 min, with 5 $^oCmin^{-1}$ heating rate. The second step was mixing the as-prepared powder with yeast (20 wt.%), an organic pore-forming agent.

2.2.3. Adsorption and kinetic experiments

Batch adsorption experiments of As^{+5}, Cr^{+6}, and phosphate ions, under magnetic mixing, was applied to evaluate effect of diffusion processes on the performance of wollastonite-based ceramics. The adsorbent material, m/V = 200 mgl^{-1} suspension, was placed in vials containing 10 ml of standard solutions of As^{+5}, Cr^{+6}, and phosphate ions at different initial concentrations, C_i, from 0.1, 0.5, 1.0, 2.5, and 5.0 mgl^{-1}, being in the range of the maximum allowable concentrations of these ions in drinking water. Maximum contaminant level of total chromium, arsenate and phosphate ions in drinking water are 0.1, 10.0, and 0.5 mgl^{-1}, respectively for public water systems [20–22]. Effect of pH was studied in the range from 3 to 10. Adsorption and kinetic experiments were performed at 25 °C. The adsorption kinetic were studied by varying the As^{+5}, Cr^{+6}, and phosphate ions solution contact time in the range 5-120 min at C_i = 1 mgl^{-1}. Mean value from three determination was used for processing of experimental data. The percentage of adsorbed As^{+5}, Cr^{+6}, and phosphate ions was calculated by using Eq. (1):

$$q = \left(\frac{C_i - C_f}{m} \right) \cdot V \tag{1}$$

where q is adsorption capacity in mgg^{-1}, C_i and C_f are initial and final As^{+5}, Cr^{+6}, and phosphate ions in mgl^{-1}, respectively, V is volume of solution in l, and m is mass of adsorbent in g.

2.3. Characterization methods

The thermal behavior and characteristic temperatures were determined by simultaneous TG–DTA (Setsys, SETARAM Instrumentation, Caluire, France) in the temperature range between 25 and 1100 ^oC, under the air flow of 20 $mlmin^{-1}$, in an Al_2O_3 pan. Based on those results, sintering regime was set up (see section 2.4.). The X-ray powder diffraction pattern was obtained using a Philips PW-1050 diffractometer with $\lambda Cu–K_\alpha$ radiation and a step/time scan mode of 0.05 $^os^{-1}$. The measurement was taken at room temperature from 10–90^o in air atmosphere. The morphology of the sintered powder was characterized by scanning electron microscopy (JEOL JSM-6390 LV). The pallets were crushed and covered with gold in order to perform these measurements.

Fourier transforms infrared spectroscopy (FTIR) spectra of the wollastonite based adsorbents were recorded in absorbance mode using a Nicolet™ iS™ 10 FT-IR Spectrometer (ThermoFisherSCIENTIFIC) spectrometer with Smart iTR™ Attenuated Total Reflectance (ATR) Sampling accessories, within a range of 400–4000 cm^{-1}, at a resolution of 4 cm^{-1} and in 20 scan mode.

Determination of textural properties of the wollastonite-based adsorbents was performed by collecting the isotherm of low-temperature nitrogen adsorption-desorption; Brunauer-Emmett-Teller (BET) and Barrett-Joyner-Halenda (BJH) methods were applied to process data. Micromeritics ASAP 2020 V4.O3 surface area and porosity analyzer was used.

2.4. Sintering process

The binder-free powders were compacted using the uniaxial double-action pressing process in an 8 mm diameter tool (Hydraulic press RING, P-14, VEB THURINGER). The applied pressure was 392 MPa, and an amount of 0.5 g of powders was used for each pressed sample. The compacts were placed in an alumna boat and heated in a tube furnace (Lenton Thermal Design Typ 1600). The compacts were sintered isothermally at 900 °C in air atmosphere for 60 min (RT–300 °C with 5 °Cmin^{-1} heating rate, 300–600 °C with 1 °Cmin^{-1} heating rate, 600–900 °C with 3 °Cmin^{-1} heating rate, 900 °C 1 h).

3. Results and discussion

3.1. Characterization of wollastonite-based adsorbent

DTA–TG curves of prepared mixture containing yeast are shown in Fig. 1. Mixture possesses two exo-thermal and one endo-thermal effects, followed by mass loss. First exo-thermal peak at around 300 °C belongs to decomposition of organic compound [23]. Mass loss that follows this decomposition process is 5 %. Sharp exo-thermal effect in the range 500–600 °C corresponds with decomposition of siloxane [24, 25]. Endo-thermal effect at around 800 °C corresponds to $CaCO_3$ decomposition [26]. Mass losses that follow $CaCO_3$ decomposition is 30 %.

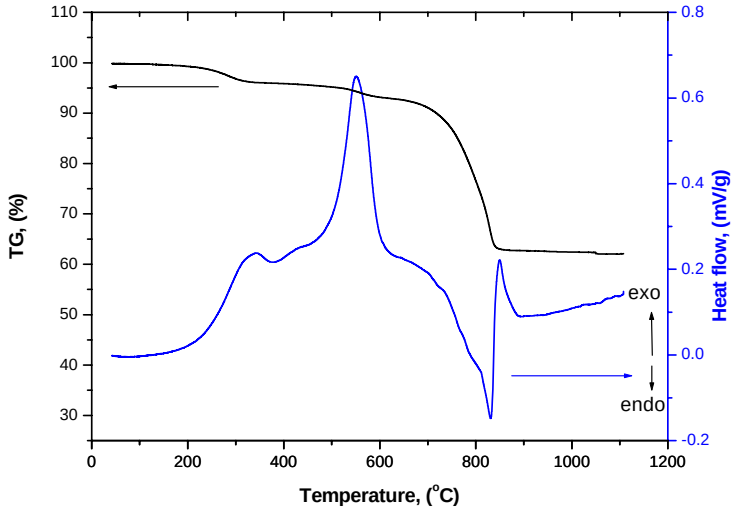

Fig. 1. DTA–TG curves of $CaCO_3$-Sil-yeast.

Based on these results, sintering regime was set up. No peaks were detected in DTA–TG curves up to 200 °C, so first part of sintering regime was non-isothermal heating from RT–300 °C, with 5 °Cmin^{-1} heating rate. All organic decompositions occur in the range from

300–600 °C, where second part of sintering regime was isothermal heating from 300–600 °C, with 1 °Cmin^{-1} heating rate. Third part of sintering regime was isothermal heating from 600–900 °C with 3 °Cmin^{-1} heating rate, due to slowly $CaCO_3$ decomposition. In order to obtain wollastonite, all samples were sintered isothermally on 900 °C for 1 h, and then cooled down to RT.

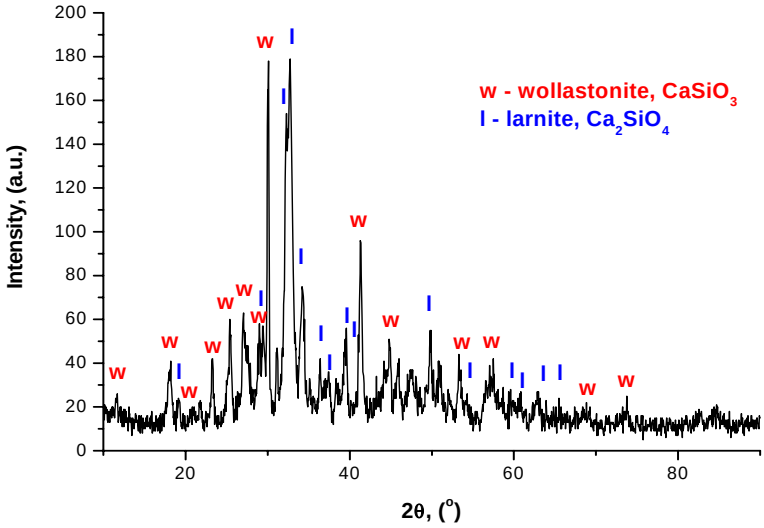

Fig. 2. XRD patterns of sintered sample $CaCO_3$-Sil-yaest.

XRD pattern of sintered samples are presented in Fig. 2. All obtained intensities were identified by JCPDS cards (042-0547 for wollastonite $CaSiO_3$, and 077-0409 for larnite Ca_2SiO_4). Two-phase system was detected: wollastonite and larnite. Mixture contains 51.1 % $CaSiO_3$, and 48.9 % Ca_2SiO_4. Sharp and intensive peaks indicate at recrystallization process.

Scanning electron micrographs of sintered samples are presented in Fig. 3. Uniform porosity is present in sintered sample. Pores are spherical, few microns in size, and inter-connected with a network of channels, approx. 1 μm in size. Besides formation of network channels, yeast makes surface erosion of wollastonite structure. Those small pores are connected with contact necks, 500–600 nm thickness. Wollastonite structure is very complex, made of agglomerates that contain pores and particles. Tough agglomerates are 400 nm sized, larger ones are present as well, but hollow and few microns sized. The agglomerates interior is consisted of nano-sized particles and great porosity. Width of agglomerates is around 200 nm**.**

ATR-FTIR analysis of $CaCO_3$-Sil-yeast sorbent confirmed wollastonite-contained ceramics structure and shows the characteristic bands at 1022 cm^{-1} and 1072 cm^{-1} originate from stretching bridging Si–O(Si), and bands at 898 cm^{-1}, 873 cm^{-1}, and 845 cm^{-1} originate from stretching non-bridging Si–O. Low intensity band at 714 cm^{-1} originates from stretching bridging Si–O(Si) which are characteristic for the presence of 3-membered ring in wollastonite-contained ceramics. The most intense band at ≈ 1460 cm^{-1} is assigned to the carbonate ion vibrational modes in bulk calcite [27].

The textural properties of the wollastonite-based adsorbent were determined using low-temperature nitrogen adsorption/desorption; the obtained textural parameters are preented in Tab. I, while the isotherm for $CaCO_3$-Sioxane-yeast sample is shown in Fig. 4. Accordingly to IUPAC classification [28], the part of isotherm between p/p_0 = 0.3 and 1 can be described as type V with a H3 type hysteresis, what can be comprehended as the indication of hierarchical structure containing both meso- and macropores, similar result has been already published in the case of wollastonite [29]. Besides, low-pressure hysteresis (p/p_0 < 0.3) indicates the existence of some microporosity. However, due to the low specific surface area, it can be supposed that porosity appears on the surface of material.

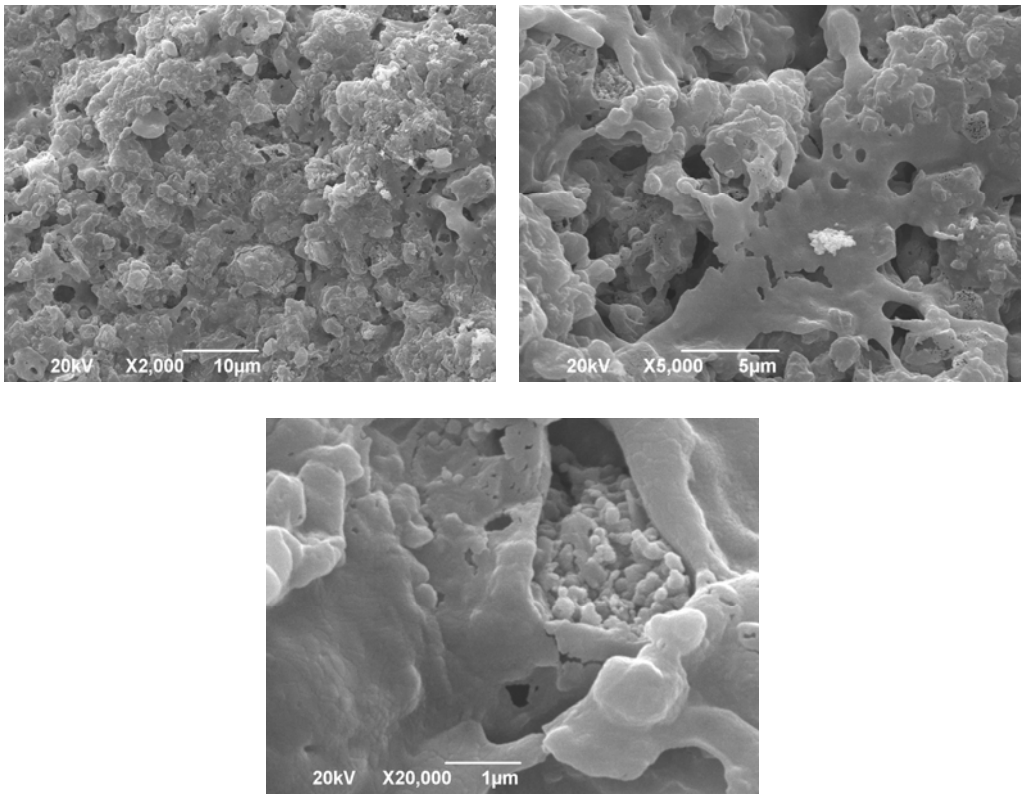

Fig. 3. SEM micrographs of sintered samples $CaCO_3$-Sil-yeast, with magnification of 2000, 5000, and 20000.

Tab. I Textural paremeters obtained by low-temperature nitrogen adsorption for sintered $CaCO_3$-Sil-yeast.

Adsorbent	Specific surface area (m^2g^{-1})	Langmuir surface area (m^2g^{-1})	Average pore volume (cm^3g^{-1})	Average pore diameter (nm)
$CaCO_3$-Sil-yeast	4.77	6.93	0.0167	14.04

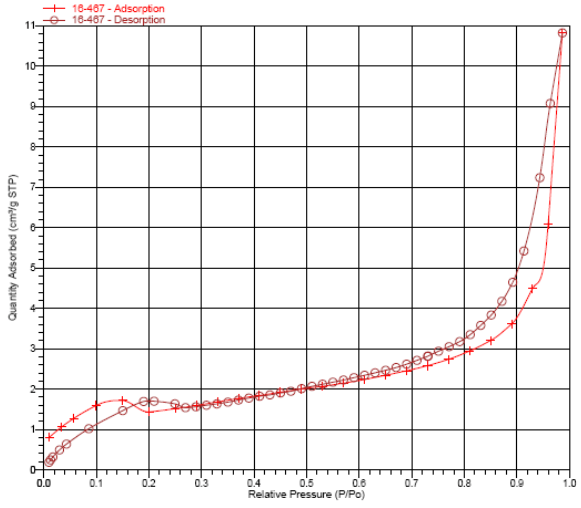

Fig. 4. BET isotherm linear plot of sintered $CaCO_3$-Sil-yeast.

3.2. Adsorption study

3.2.1. Effect of pH on adsorption efficiency

The pH influences state of equilibrium of ionic sorbate species and protonation/deprotonation of the functional groups present at adsorbent surface. It is known that presence of hydrogen/hydroxide ion could modify the redox potential of both sorbates and sorbents, and provoke dissolution of the sorbent. The results of the determination of influence of pH on adsorption efficiency of As^{+5}, Cr^{+6}, and phosphate ions indicated that adsorption of As^{+5}, Cr^{+6}, and phosphate ions on $CaCO_3$-Sil-yeast sorbent was independent in the pH range 4–8 with > 90 % removal. Decrease of As^{+5} removal was observed at pH>8. According to pH-dependent ionization of triprotic weak arsenic acid (H_3AsO_4), *i.e*. pKa(1) of 2.3, pKa(2) of 7.0, and pKa(3) of 11.5, it was proved that in the range of highest adsorption As^{+5} ionic species shows the most effective removal at pH in the vicinity of p*K*a. Positively charged adsorbent surface attracts the negatively charged sorbate ions by electrostatic interactions contributing to more efficient arsenic removal. Electrostatic repulsion between negatively charged arsenate species, $H_2AsO_4^-$ and $HAsO_4^{-2}$ ions, and adsorbent surface at higher pH contribute to decrease of adsorption efficiency. Similar behavior stand for Cr^{+6}, and phosphate in the studied pH range. Selection of optimal pH value 6 for As^{+5} and phosphate removal, and pH 5 for Cr^{+6} was made, and these pH was used throughout of adsorption experiments.

3.2.2. Adsorption study

The state of adsorption equilibrium can be described by fitting experimental data with various adsorption isotherms [30], and statistical criteria used to evaluate the quality of model fitting of adsorption data. Since the linear regression lines, obtained using Langmuir 1 adsorption isotherms, have highly significant correlation coefficients ($R^2 > 0.992$ for all As^{+5}, Cr^{+6}, and phosphate ions adsorption) it indicate a good fit to the Langmuir 1 equation. The values of Langmuir 1 adsorption isotherm parameters at 25 °C for As^{+5}, Cr^{+6}, and phosphate ions adsorption using $CaCO_3$-Sil-yeast sorbent, are presented in Tab. II. The Langmuir 1 isotherm model is given by Eq. (2) and linearized form, by Eq. (3):

$$q_e = \frac{\left(b \cdot q_{\max} \cdot C_e\right)}{\left(1 + b \cdot C_e\right)} \tag{2}$$

$$\frac{C_e}{q_e} = \frac{1}{b \cdot q_{\max}} + \frac{C_e}{q_{\max}} \tag{3}$$

where: C_e is the equilibrium concentration of As^{+5}, Cr^{+6}, and phosphate ions remaining in the solution ($mol l^{-1}$); q_e is the amount of ions sorbed per weight unit of solid at equilibrium ($mol g^{-1}$); b is Langmuir constant related to sorption affinity, and q_{max} is maximum sorption capacity ($mol g^{-1}$).

Tab. II Langmuir 1 adsorption isotherm parameters at 25 °C for As^{+5}, Cr^{+6}, and phosphate ions adsorption using $CaCO_3$-Sil-yeast sorbent.

Langmuir 1 isotherm parameters	$CaCO_3$-Sil-yeast sorbent		
	Cr^{+6}	phosphate ions	As^{+5}
q_e ($mg g^{-1}$)	21.858 ±1.021	15.285 ±1.014	39.966±0.950
b ($l mg^{-1}$)	27.742 ±0.820	110.920 ±1.028	45.610±0.920
b ($l mol^{-1}$)	1442323±915	3435246±1014	3417650±1035
R^2	0.992±0.022	0.998±0.010	0.986±0.012

High adsorption capacities: 21.858 mgg^{-1} for Cr^{+6}, 15.285 mgg^{-1} for phosphate, and 39.966 mgg^{-1} for As^{+5} were obtained for $CaCO_3$-Sil-yeast sorbent.

3.2.3. Effect of time on adsorption capacity

The removal of As^{+5}, Cr^{+6}, and phosphate ions by adsorption on $CaCO_3$-Sil-yeast increased with time up to 90 min; thereafter it became constant.The kinetic parameters of As^{+5}, Cr^{+6}, and phosphate ions adsorption, presented in Tab. III, showed that $CaCO_3$-Sil-yeast sorbent possess high affinity with respect to As^{+5}, Cr^{+6}, and phosphate ions, and satisfactory rate at which system attain equilibrium.

Tab. III Kinetic parameters obtained by the use of Lagergren algorithm and W-M model for $CaCO_3$-Sil-yeast sorbent at 25 °C, C_0 = 1.0 mgl^{-1}, m/V = 200 mgl^{-1}.

Pseudo-second order	Cr^{+6}	Phosphate ions	As^{+5}
k_2x10^2 ($gmg^{-1}min^{-1}$)	0.577	1.834	3.4184
q_e (mgg^{-1})	5.314	5.246	5.373
R^2	0.961	0.944	0.936
W-M model fitting			
Step 1- Intra-particle diffusion	Cr^{+6}	Phosphate ions	As^{+5}
k_{p1} ($mgg^{-1}min^{-0.5}$)	0.4304	0.5534	0.4698
C (mgg^{-1})	1.4454	1.3978	1.3936
R^2	0.974	0.991	0.983
Step 2 - Equilibrium	Cr^{+6}	$H_2PO_4^-$	As^{+5}
k_{p2} ($mgg^{-1}min^{-0.5}$)	0.0419	0.0239	0.0065
C (mgg^{-1})	4.4714	4.721	4.961
R^2	0.989	0.910	1

The analysis of kinetic data, using pseudo-second-order kinetic method, resulted in significantly higher second-order rate constant and similar adsorption capacity values for As^{+5} adsorption compare with Cr^{+6}, and phosphate ions adsorption using $CaCO_3$-Sil-yeast sorbent. Kavitha and co-workers found that results of kinetic parameters of the adsorption of Cr^{+6} on wollastonite based adsorbent (quartz/ feldspar/wollastonite - QFW) is best described by the pseudo-second order equation suggesting that the rate-limiting step may be the adsorption mechanism but not mass transport [31]. Results of intra-particle Weber–Morris diffusion model showed two step adsorption process with fast kinetic in first step for As^{+5}, Cr^{+6}, and phosphate ions adsorption.

First kinetic step demonstrates external mass transfer from bulk solution, related not only to instantaneous adsorbate bonding at the most readily available adsorbing sites at outer surface, but also could be due to the contribution of adsorption at surface of the pores with largest diameter close to the particle surface [32]. While in the course of final stage, i.e. second step, slow transport of As^{+5}, Cr^{+6}, and phosphate ions inside micro pores dominate and attainment of adsorption/desorption equilibrium denote overall saturation of available adsorptive sites.

Various solid materials including activated carbons, silica gels, activated clays, activated alumina and other oxides, zeolites, bauxite, different biosorbents have been used for As^{+5}, Cr^{+6}, and phosphate ions removal from waters. The application of wollastonite based adsorbents was reported in literature as well. As^{+5}, Cr^{+6}, and phosphate ions adsorption capacities (value of q_e derived from Langmuir equation) of various wollastonite based adsorbents are summarized in Tab. IV.

Tab. IV Comparison of adsorbents.

Adsorbent	Ion	Concentration, mgl^{-1}	$q_{e,\ mgl}{}^{-1}$	reference
QFW	Cr^{+6}	10	9.81	[31]
Wollastonite	Cr^{+6}	2.6	0.69	[33]
Wollastonite	Cr^{+6}	5.0	21.92	[34]
Wollastonite	As^{+5}	5.0	23.88	[34]
Wollastonite	phosphate ions	5.0	27.29	[34]

Importantly, the adsorption capacities of wollastonite-based materials used in this work are similar or in the same range of values as those already reported for other materials: the insight into literature data reveals that capacities for Cr^{6+} [35], As^{5+} [36–38], or phosphate ions [39, 40] are in the range of units or tens of mgg^{-1}, what is comparable with the results reported in this work.

4. Conclusion

Porous wollastonite-based ceramics were synthesized using yeast as a porogen agent in order to obtain appropriate porosity of obtained adsorbents. DTA gave us characteristic temperatures, we chose appropriate sintering regime up to 900 ^{o}C. XRD measurements confirmed wollastonite phase, while SEM confirmed macro and micro porosity. Synthesized $CaCO_3$-Siloxane-yeast sorbent was used for As^{+5}, Cr^{+6}, and phopshate removal, and results showed that pH is important parameter which control effectiveness of pollutant removal.
The quality of the isotherm modeling of adsorption data was judged by the correlation coefficients and error functions, and the best adsorption model was found to be Langmuir isotherm. Time dependent study showed that the best fitting kinetic model is parabolic or Weber-Morris model giving the highest values of correlation coefficients than the other investigated models. The kinetic data of the sorption was well fitted with the pseudo-second-order kinetic and Weber-Morris models, suggesting that the rate-limiting step was diffusion rather than chemical sorption.

Acknowledgement

This research was performed within the bilateral cooperation between Serbia and France, N^{o} 4510339/2016/09/03 "*Inteligent eco-nanomaterials and nanocomposites*". The authors are grateful to Dr. Miodrag Mitrić for XRD measurement, and Dr. Smilja Marković for DTA-TG measurement.

5. References

1. R. A. Rashid, R. Shamsudin, M. A. A. Hamid, A. Jalar, Low temperature production of wollastonite from limestone and silica sand through solid-state reaction, Journal of Asian Ceramic Societies, 2 (2014) 77–81.
2. J. H. Jean, C. R. Chang, C. D. Lei, Sintering of a crystallisable $CaO–B_2O_3–SiO_2$ glass with silver, Journal of American Ceramic Society, 87 (2004) 1244–1249.
3. N. S. Negmatov, Z. Zh. Abdullaev, High-voltage electric insulators based on wollastonite, Glass Ceramics, 58 (2001) 396–397.

4. H. R. Manouchehri, K. H. Rao, K. S. E. Forssberg, Triboelectric charge, electrophysical properties and electrical beneficiation potential of chemically treated feldspar, quartz and wollastonite, Magnetic & Electrical Separation, 11 (2002) 9–32.
5. W. Xue, X. Liu, X. B. Zheng, C. Ding, In vivo evaluation of plasma-sprayed wollastonite coating, Biomaterials, 26 (2005) 3455–3460.
6. H. Maeda, T. Okuyama, E. H. Ishida, T. Kasuga, Preparation of porous spheres containing wollastonite by an electrospray method, Materials Letters, 95 (2013) 107–109.
7. A. R. Studart, U. T. Gonzenbach, E. Tervoort, L. J. Gauckler, Processing Routes to Macroporous Ceramics: A Review, Journal of American Ceramic Society, 89 (6) (2006) 1771–1789.
8. P. Wu, Y. Xu, Z. Huang, J. Zhang, A review of preparation techniques of porous ceramic membranes, Journal of Ceramic Processing Research, 16 (2015) 102–106.
9. J. G. Ayala-Landeros, V. Saucedo-Rivalcoba, S. Bribiesca-Vasquez, V. M. Castaño, A. L. Martínez-Hernández, C. Velasco-Santos, Influence of Corn Flour as Pore Forming Agent on Porous Ceramic Material Based Mullite: Morphology and Mechanical Properties, Science of Sintering, 48 (2016) 29–39.
10. Gary R. Pickrell, Porous ceramic, polymer and metal materials with pores created by biological fermentation, US patent 2006/0008634 A1.
11. R. G. Carrodegeus, A. H. De Aza, P. N. De Aza, C. Baudin, J. Jimenez, A. Laopez-Bravo, P. Pena, S. De Aza, Assessment of natural and synthetic wollastonite as source for bioceramics preparation, Journal of Biomedical Materials Research A, 83 (2007) 484–495.
12. K. Lin, W. Zhai, S. Ni, J. Chang, Y. Zeng, W. Qian, Study of the mechanical property and in vitro biocompatibility of $CaSiO_3$ ceramics, Ceramics International, 31 (2005) 323–326.
13. L. H. Long, L. D. Chen, S. Q. Bai, J. Chan and K. L. Lin, Preparation of dense β-$CaSiO_3$ ceramic with high mechanical strength and HAp formation ability in simulated body fluid, Journal of the European Ceramic Society, 26 (2006) 1701–1706.
14. M. A. De la Casa-lillo, P. Velasquez and P. N. De Aza, Influence of thermal treatment on the “in vitro” bioactivity of wollastonite materials, Journal of Materials Science: Materials in Medicine, 22 (2011) 907–915.
15. E. Bernardo, P. Colombo, I. Cacciotti, A. Bianco, R. Bedini, R. Pecci, K. Pardun, L. Treccani, K. Rezwan, Porous wollastonite–hydroxyapatite bioceramics from a preceramic polymer and micro- or nano-sized fillers, Journal of the European Ceramic Society, 32 (2012) 399–408.
16. G. Xua , J. Li , H. Cui, Q. He, Z. Zhang, X. Zhan, Biotemplated fabrication of porous alumina ceramics with controllable pore size using bioactive yeast as pore-forming agent, Ceramics International, 41 (2015) 7042–7047.
17. Y. Ma, Q. L. Wei, R. W. Ling, F. K. An, G. Y. Mu, Y. M. Huang, Synthesis of macro-mesoporous alumina with yeast cell as bio-template, Microporous Mesoporous Mater., 165 (2013) 177–184.
18. G. G. Xu, Y. H. Ma, H. Z. Cui, G. Z. Ruan, Z. H. Zhang, H. L. Zhao, Preparation of porous mullite-corundum ceramics with controlled pore size using bioactive yeast as pore-forming agent, Materials Letters, 116 (2014) 349–352.
19. E. Slavikova, R. Vadkertiova, The diversity of yeasts in the agricultural soil, Journal of Basic Microbiology, 43 (2003) 430–436.
20. Agency for Toxic Substances and Disease Registry, Case Studies in Environmental Medicine (CSEM), Chromium Toxicity, Available at: https://www.atsdr.cdc.gov/csem/chromium/docs/chromium.pdf .

21. M. Kumar, A. Puri, A review of permissible limits of drinking water, Indian Journal of Occupational and Environmental Medicine, Vol 16, Issue 1, DOI: 10.4103/0019-5278.99696.
22. I. A. Kumar, N. Viswanathan, Fabrication of metal ions cross-linked alginate assisted biocomposite beads for selective phosphate removal, Journal of Environmental Chemical Engineering, http://dx.doi.org/10.1016/j.jece.2017.02.005, In Press
23. M. H. Soliman, A. M. M. Hindy, G. G. Mohamed, Thermal decomposition and biological activity studies of some transition metal complexes derived from mixed ligands sparfloxacin and glycine, Journal of Thermal Analysis and Calorimetry, 115 (2014) 987–1001.
24. J. Green, Carborane-Siloxane Elastomers, Thiokol Reaction Motors Division, 1966.
25. A. Jitianu, K. Lammers, G. A. Arbuckle-Kiel, L. C. Klein, Thermal analysis of organically modified siloxane melting gels, Journal of Thermal Analysis and Calorimetry, 107 (2012) 1039–1045.
26. I. Halikia, L. Zoumpoulakis, E. Christodoulou, D. Prattis, Kinetic study of the thermal decomposition of calcium carbonate by isothermal methods of analysis, The European Journal of Mineral Processing and Environmental Protection, 1 (2) (2001) 89–102.
27. H. A. Al-Hosney, V. H. Grassian, Water, sulfur dioxide and nitric acid adsorption on calcium carbonate: A transmission and ATR-FTIR study, Physical Chemistry Chemical Physics, 7 (2005) 1266–1276.
28. K. S. W. Sing, D. H. Everett, R. A. W. Haul, L. Moscou, R. A. Pierotti, J. Rouquerol, T. Siemieniewska, Reporting Physisorption Data For Gas/Solid Systems with Special Reference to the Determination of Surface Area and Porosity. Pure & Appl. Chem., 57, No. 4, (1985) 603–619.
29. W. Xue, A. Bandyopadhyay, S. Bose, Mesoporous calcium silicate for controlled release of bovine serum albumin protein. Acta Biomaterialia, 5 (2009) 1686–1696.
30. K. Y. Foo, B. H. Hameed, Insights into the modeling of adsorption isotherm systems, Chemical Engineering Journal, 156 (1) (2010) 2–10.
31. B. Kavitha, D. S. Thambavani, Kinetics, equilibrium isotherm and neural network modeling studies for the sorption of hexavalent chromium from aqueous solution by quartz/feldspar/wollastonite, RSC Adv., 2016, 6, 5837, DOI: 10.1039/c5ra22851d.
32. J. Markovski, D. Marković, V. Đokić, M. Mitrić, M. Ristić, A. Onjia, A. Marinković, Arsenate adsorption on waste eggshell modified by goethite, α-MnO_2 and goethite/α-MnO_2, Chemical Engineering Journal, 237 (2014) 430–442.
33. Y. C. Sharma, V. Srivastava, J. Srivastava, M. Mahto, Reclamation of Cr(VI) rich water and wastewater by wollastonite, Chemical Engineering Journal, 127 (2007) 151–156, doi:10.1016/j.cej.2006.09.012.
34. Nina Obradović, Suzana Filipović, Smilja Marković, Miodrag Mitrić, Jelena Rusmirović, Aleksandar Marinković, Vesna Antić, Vladimir Pavlović, Influence of different pore-forming agents on wollastonite microstructures and adsorption capacities, Ceramics International, Article in Press, http://dx.doi.org/10.1016/j.ceramint.2017.03.021.
35. Claudia Rosales-Landeros, Carlos Eduardo Barrera-Díaz, Bryan Bilyeu, Víctor Varela Guerrero, Fernando Urena Núnez; A Review on Cr(VI) Adsorption Using Inorganic Materials, American Journal of Analytical Chemistry, 4 (2013) 8–16.
36. Nina Ricci Nicomel, Karen Leus, Karel Folens, Pascal Van Der Voort and Gijs Du Laing; Technologies for Arsenic Removal from Water: Current Status and Future Perspectives, Int. J. Environ. Res. Public Health, 13 (2016) 62.
37. Shuhua Yao, Ziru Liu and Zhongliang Shi; Arsenic removal from aqueous solutions by adsorption onto iron oxide/activated carbon magnetic composite, Journal of Environmental Health Science and Engineering, 12 (2014) 58.

38. E. N. Bakatula, R. Molaudzi, P. Nekhunguni, H. Tutu; The Removal of Arsenic and Uranium from Aqueous Solutions by Sorption onto Iron Oxide-Coated Zeolite (IOCZ). Water, Air, & Soil Pollution January 228 (2017) 5.
39. Mengxue Li, Jianyong Liu, Yunfeng Xu, and Guangren Qian; Phosphate adsorption on metal oxides and metal hydroxides: A comparative review. Environ. Rev., 24 (2016) 1–14.
40. Weiya Huang, Yuanming Zhang, Dan Li; Adsorptive removal of phosphate from water using mesoporous materials: A review. Journal of Environmental Management, 193 (2017) 470–482.

Садржај: *У овом раду, синтетисана је порозна керамика на бази воластонита. За почетне материјале, узети су керамички прекурсор, метилхидроксициклосилоксан, и микронски прах $CaCO_3$. Након 20 min ултразвучног третмана и калцинације од пола сата на 250 ^oC, у тако добијене прахове додат је квасац, као пороген. Режим синтеровања је одређен на основу резултата добијених ДТА анализом. Припремљене смеше су испресоване и синтероване на 900 ^oC, 1 h. Након процеса синтеровања, добијена је порозна керамика на бази воластонита. Фазни састав и микроструктура одређени су рендгенском дифракцијом и скенирајућом електронском микроскопијом. Изучаван је утицај pH вредности, контактног времена и концентрације јона на ефикасност адсорпције јона As^{+5}, Cr^{+6} и фосфата. Зависност адсорпције од времена најбоље описује кинетички модел псеудо другога реда и модел Weber-Morris, који предвиђа интра-честичну дифузију као контролу брзине читавог процеса. Измерени су високи адсорпциони капацитети, 39,97, 21,87 и 15,29 mgg^{-1} за As^{+5}, Cr^{+6} и фосфатне јоне, тим редом.*

Кључне речи: *квасац, синтеровање, порозна керамика на бази воластонита.*